
Quality Sentinel: Estimating Label Quality and Errors in Medical Segmentation Datasets

Yixiong Chen, Zongwei Zhou*, Alan Yuille
Johns Hopkins University

Abstract

An increasing number of public datasets have shown a transformative impact on automated medical segmentation. However, these datasets are often with varying label quality, ranging from manual expert annotations to AI-generated pseudo-annotations. There is no systematic, reliable, and automatic quality control (QC). To fill in this bridge, we introduce a regression model, Quality Sentinel, to estimate label quality compared with manual annotations in medical segmentation datasets. This regression model was trained on over 4 million image-label pairs created by us. Each pair presents a varying but quantified label quality based on manual annotations, which enable us to predict the label quality of any image-label pairs in the inference. Our Quality Sentinel can predict the label quality of 142 body structures. The predicted label quality quantified by Dice Similarity Coefficient (DSC) shares a strong correlation with ground truth quality, with a positive correlation coefficient ($r = 0.902$). Quality Sentinel has found multiple impactful use cases. (I) We evaluated label quality in publicly available datasets, where quality highly varies across different datasets. Our analysis also uncovers that male and younger subjects exhibit significantly higher quality. (II) We identified and corrected poorly annotated labels, achieving 1/3 reduction in annotation costs with optimal budgeting on TotalSegmentator. (III) We enhanced AI training efficiency and performance by focusing on high-quality pseudo labels, resulting in a 33%–88% performance boost over entropy-based methods, with a cost of 31% time and 4.5% memory. The [data and model](#) are released.

1 Introduction

Recent advances in large-scale organ segmentation [Liu et al., 2023] have shown significant potential for developing foundational models for general medical segmentation tasks. The datasets [Wasserthal et al., 2023, Jaus et al., 2023, Qu et al., 2024], which comprise thousands of 3D scans covering numerous organs, facilitate the training of powerful and generalizable models. However, the annotation process for most of these datasets involves AI-assisted methodologies [Budd et al., 2021], resulting in a predominance of model-generated pseudo labels. The inherent label noise can adversely affect the scalability and performance of the datasets. The models trained on these datasets may also lack reliability. Consequently, there is a critical need for a quality control (QC) method to make the annotation quality accessible, so that both the data quality and model performance can be improved.

The primary approach to controlling label quality involves radiologists’ manual inspection. However, this is subjective and becomes increasingly time-consuming and impractical with the data growth, such as the AbdomenAtlas 1.1 [Li et al., 2023], which contains 3.7 million CT slices. Automatic methods for estimating pseudo label quality typically rely on the entropy of model predictions [Culotta and McCallum, 2005, Mahapatra et al., 2018] (*i.e.*, uncertainty) and the inconsistency of

*Corresponding author: Zongwei Zhou (zzhou82@jh.edu)

prediction among multiple models [Li and Guo, 2013, Gal et al., 2017] (*i.e.*, diversity). However, these methods present significant drawbacks. Firstly, a model’s feedback reflects its own confidence rather than the actual label quality. Secondly, the metrics are class-dependent (*e.g.*, organs with larger volumes exhibit higher entropy), which complicates the comparison of label quality across classes.

To address the challenges of accurately and efficiently measuring label quality under a uniform standard across all classes, we have devised a framework that trains models specifically for estimating the quality of labels (masks) in organ segmentation tasks. This framework employs the DSC, a comparison between the current label and the gold standard (ground truth), as the predictive metric for label quality. We refer to the models trained within this framework as **Quality Sentinel**. In previous literature on label evaluation models [Huang et al., 2016, DeVries and Taylor, 2018, Galdran et al., 2018, Zhang et al., 2021, Zhou et al., 2023], the common practice is using an image-label pair as the input and predicting a quality metric. They are typically trained on a single or small collection of organs, hindering their practical use on modern multi-organ segmentation datasets. What sets Quality Sentinel apart from existing methods is it incorporates large language models to identify target organs, enhancing its performance in images featuring multiple organs. Specifically, we utilize the pretrained Contrastive Language-Image Pre-training (CLIP) [Radford et al., 2021] text encoder to embed the text description of 142 organs. This serves as a conditional input, allowing the model to recognize the organ it is evaluating. Furthermore, we introduce a scale-invariant ranking loss to overcome the challenges associated with training Quality Sentinel, a regressor, on a skewed DSC distribution. This not only facilitates smoother training but also significantly boosts its ranking accuracy. In summary, our work presents three major **contributions** to the field of medical image segmentation and dataset evaluation.

- First, we introduce Quality Sentinel, a novel medical segmentation evaluation model designed to estimate label quality through DSC prediction. This model is distinguished by its use of text embeddings as conditions for different classes and a novel ranking loss mechanism, enabling effective multi-organ segmentation evaluation (Sect. 3, Fig. 1).
- Second, we apply Quality Sentinel to reveal a large label quality variability among datasets. It also uncovers notable gender and age disparities in annotation quality. Specifically, labels associated with female and older patients exhibit lower quality, highlighting the need for increased diligence in dataset construction to mitigate the annotation biases, especially for these groups (Sect. 4.3, Tab. 2, Fig. 5).
- Third, we demonstrate the efficacy of Quality Sentinel as a sample selector for training segmentation models. It outperforms traditional diversity and uncertainty-based methods. On the one hand, it enhances the data efficiency in the human-in-the-loop process (active learning) for dataset development. On the other hand, by selecting high-quality pseudo labels in semi-supervised training, the segmentation models can be more reliable and powerful (Sect. 4.4, Fig. 6, Tab. 3).

2 Related Work

2.1 Multi-Organ Segmentation

With the rapid advances of deep segmentation models [Ronneberger et al., 2015, Isensee et al., 2021, Oktay et al., 2018, Chen et al., 2021, Hatamizadeh et al., 2022, Tang et al., 2022] and the emergence of large-scale multi-organ segmentation datasets [Ji et al., 2022, Ma et al., 2021, Wasserthal et al., 2023], the need for data processing, filtering, and corresponding model training strategies has also grown. The existing dataset with the largest sample size is AbdomenAtlas [Qu et al., 2024]. It labels 32 organs and tumors over 9,000 3D CT volumes with a human-in-the-loop technique. This method accelerates the annotation process to a large extent (as reported, the dataset was annotated within three weeks), but the high ratio of AI-generated pseudo labels may also make the dataset potentially risky in low-quality annotations. TotalSegmentator [Wasserthal et al., 2023], a large dataset with 1,000+ samples and 100+ classes, relies upon quality insurance via 3D renderings and expert checks. The labor-intensive checking results in the final checking rate of only 100 CT volumes. To this end, an efficient QC tool to ensure annotation quality is in urgent need.

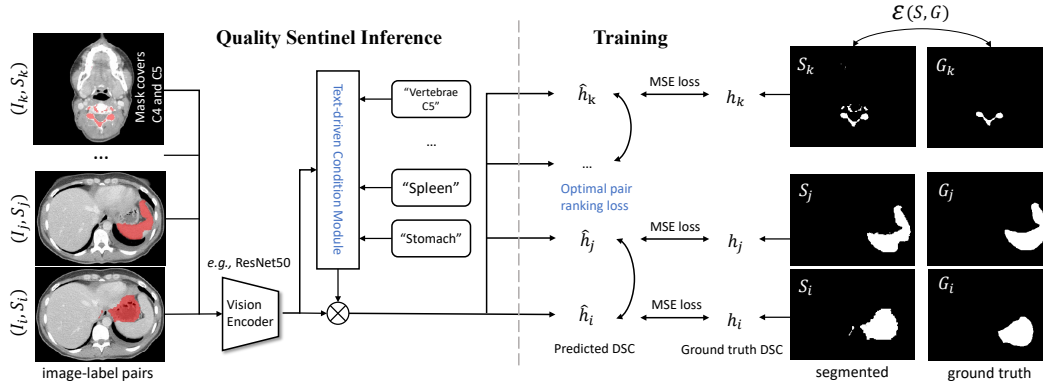


Figure 1: Overview of Quality Sentinel: Inputs are image-label pairs with pseudo labels. It employs a vision encoder to estimate DSC relative to ground truths. The Text-driven Condition Module encodes texts to augment the model for organ identification, addressing the ambiguity of organ-label matching (e.g., for (I_k, S_k) at upper left, the mask covers two organs). Training involves a compositional loss, combining optimal pair ranking and MSE, to align predicted with actual DSC.

2.2 Medical Segmentation Quality Control

QC tools raise a flag when the segmentation model under analysis incurs a lack of reliability or robustness [Galati et al., 2022]. They can be categorized into two folds: the pre-analysis and the post-analysis QC. Pre-analysis QC [Lorch et al., 2017, Tarroni et al., 2018, Oksuz et al., 2019] performs on the input of the segmentation model, it emulates expert criteria and detects low-quality samples (e.g., incomplete or corrupted scans). By giving binary feedback, it can discard those samples to improve the robustness of the segmentation pipeline. Post-analysis QC [Alba et al., 2018, Robinson et al., 2018, Lin et al., 2022] focuses on the assessment of the segmentation outputs of a model. It usually infers common segmentation metrics (e.g., DSC, Hausdorff Distance (HD), or uncertainty estimates), thus detecting a malfunction of models. Quality Sentinel is a tool that can serve as both pre-analysis and post-analysis. On the one hand, it helps to detect flaws in the existing datasets by analysis of the label quality. On the other hand, it can evaluate model outputs and find the weaknesses of the model, which can be beneficial for further refinement. Moreover, existing QC techniques primarily work on single organs (e.g., Cardiac MR [Lorch et al., 2017, Tarroni et al., 2018, Oksuz et al., 2019, Alba et al., 2018, Robinson et al., 2018]) or a small set of relevant organs (e.g., knee and calf muscle [Zaman et al., 2023]). Quality Sentinel is an exploration of general-purpose QC tool that works for a wide variety of organs simultaneously.

2.3 Language-driven Medical Image Analysis

Large language models [Devlin et al., 2019, Brown et al., 2020] widely succeed in language processing and understanding. Visual language models (VLMs) [Wang et al., 2022] such as CLIP have been explored to promote medical image analysis tasks such as medical vision question answering [Eslami et al., 2023], medical object recognition [Qin et al., 2022], and organ/tumor segmentation [Liu et al., 2023, Ulrich et al., 2023]. VLM could be useful in these scenarios because the language encoder can generate intrinsic semantics of the anatomical structures for tasks in the medical domain with carefully designed medical prompts. Therefore, the vision module can be augmented with knowledge from the language domain. For Quality Sentinel, the text embedding acts as the condition for the vision representation of a target class, and similar classes share similar knowledge from language.

3 Quality Sentinel

3.1 Formulation of the Quality Estimation Framework

The Quality Sentinel framework, depicted in Fig. 1, evaluates data batches of N samples, denoted as $\mathcal{D} = \{I_i, S_i, G_i\}_{i=1}^N$, where I , S , and G represent an image, a segmented mask (pseudo label),

and a ground truth label, respectively. The estimation model \mathcal{Q} , parameterized by θ , estimates the DSC $\hat{h}_i = \mathcal{Q}(I_i, S_i; \theta)$, compared against the actual DSC $h_i = \mathcal{E}(S_i, G_i)$. To align the predicted \hat{h} with the actual h , we introduce a compositional loss function:

$$\mathcal{L} = \frac{1}{N} \sum_{i=1}^N \mathcal{L}_{MSE}(\hat{h}_i, h_i) + \lambda \mathcal{L}_{Rank}(\hat{\mathbf{h}}, \mathbf{h}), \quad (1)$$

with λ as a scaling constant. The mean square error (MSE) loss $\mathcal{L}_{MSE}(\hat{h}_i, h_i)$ aims to match the model’s output with the ground truth DSC. The novel optimal-pair ranking loss $\mathcal{L}_{Rank}(\hat{\mathbf{h}}, \mathbf{h})$ enhances the model’s ranking capability by optimizing the order of predicted and actual DSC within the batch \mathcal{D} .

For practical application, we process a 2D image-label pair as input to \mathcal{Q} , averaging estimates from 10 uniformly sampled 2D slices along the z-axis for 3D organ label quality estimation. This 2D-based method is superior to 3D methods because slice-level prediction is more accurate and can provide clinicians with specific information related to the single slices [Fournel et al., 2021].

3.2 Text-driven Condition Module

Challenges arise with expanded or fragmented masks during the segmentation of small or irregularly shaped organs, as seen in the upper left of Fig. 1 (a mask covers two organs), causing ambiguity in organ-label matching. This ambiguity compromised the evaluation model’s accuracy. To address this, Quality Sentinel employs CLIP text embeddings of organ classes as conditions to discern the target organ amidst multiple organs within an image. The text embeddings also encourage the model to learn shared representations for similar classes due to their similar conditions. In this way, similar classes can learn similar evaluation criteria and promote each other’s performance.

As for the generation of text embeddings, it is crucial to choose an appropriate prompt template [Qin et al., 2022] because it is the key to eliciting knowledge from pre-trained VLMs. According to our ablation study in Section 4.2, the best prompt is “[CLS]”, the class name itself.

Quality Sentinel views text embeddings as class-conditional attention added before the decision layers. For a given class k , its CLIP text embedding φ_k is concatenated with the image feature $f_1 = E_v(x)$ produced by a vision encoder (*e.g.*, ResNet50 [He et al., 2016]). A multi-layer perceptron (MLP) then computes attention weights $[\omega_1, \omega_2] = MLP([f_1, \varphi_k])$, used by the regression prediction head, consisting of two fully connected (FC) layers $g_1(\cdot)$ and $g_2(\cdot)$, to make the final prediction:

$$\hat{h} = g_2(\omega_2 \otimes g_1(\omega_1 \otimes E_v(x))), \quad (2)$$

where \otimes denotes element-wise multiplication. Employing two FC layers allows for a phased feature compression, enabling the attention mechanism to more significantly influence prediction outcomes.

3.3 Optimal Pair Ranking Loss

Reliance on MSE loss alone is inadequate for training Quality Sentinel due to its tendency to bias DSC predictions towards the most common score interval. Considering the framework’s application in ranking sample quality and selecting pseudo labels for revision, we introduce a scale-insensitive ranking loss as an auxiliary training mechanism.

Inspired by the approach in [Yoo and Kweon, 2019], we compare sample pairs. However, in the context of multi-organ segmentation, comparing dissimilar organ classes (*e.g.*, spleen vs. skull) is unproductive. Thus, we form $N/2$ pairs within a batch of size N , ensuring each pair consists of identical or similar class samples by maximizing their total embedding similarity. The pairing process involves three steps: 1) computing a cosine similarity matrix $H \in \mathbb{R}^{N \times N}$; 2) converting H into a cost matrix $H' = -H + \infty \cdot I_{N \times N}$ to prevent self-pairing; 3) identifying optimal pairs through the Jonker-Volgenant algorithm for linear sum assignment [Crouse, 2016].

For an optimal pair $\{x^p = \{x_i, x_j\}\}$, the ranking loss is:

$$\mathcal{L}_{Rank}(\hat{h}_i, \hat{h}_j, h_i, h_j) = \max(0, (\hat{h}_i - \hat{h}_j) \cdot (h_j - h_i) + \xi), \quad (3)$$

where ξ is a predefined positive margin. This loss specifically penalizes discrepancies in the directional agreement between the predicted and actual DSC differences.

Table 1: Ablation study for Quality Sentinel. The baseline is a ResNet50 with MSE loss. All results are reported on the resampled testing set.

Condition	Opt. Pair Loss	Data Resampling	LCC	SROCC	MAP@5	MAP@10
-	-	-	0.797	0.775	0.417	0.481
One-hot	-	-	0.817	0.795	0.427	0.501
CLIP: "A computerized tomography of a [CLS]."	-	-	0.840	0.805	0.438	0.510
CLIP: "There is [CLS] in this computerized tomography."	-	-	0.847	0.801	0.444	0.525
CLIP: "A photo of a [CLS]."	-	-	0.852	0.808	0.445	0.533
CLIP: "[CLS]"	-	-	0.853	0.808	0.449	0.531
-	✓	-	0.817	0.778	0.438	0.535
CLIP: "[CLS]"	✓	-	0.855	0.810	0.463	0.546
CLIP: "[CLS]"	✓	✓	0.902	0.856	0.500	0.565

4 Experiments & Results

4.1 Experimental Settings

Stage 1 Dataset Construction. We fine-tuned the pretrained STUNet [Huang et al., 2023] on the DAP Atlas [Jaus et al., 2023], a comprehensive dataset that aggregates 142 categories from 14 datasets. Model checkpoints were saved at specified epochs: 10, 20, 30, 40, 50, 100, 200, 300, 400, 500. From each checkpoint, pseudo labels for 15 CT scans were generated, with 10 designated for training and 5 for testing, creating a dataset of CT scans paired with pseudo labels of varying quality and their corresponding ground truth DSC. Because DAP Atlas is also an AI-assisted dataset, its ground truth masks may not be accurate enough. Therefore, these imperfect ground truths cannot serve as the training samples with $DSC = 1.0$. The generated masks and their DSCs are feasible to train the model because their variations are minimized when averaged over the large dataset. To further decrease the inaccuracy of ground truth DSC for training, we resample data to refine their quality.

Stage 2 Data Resampling. Utilizing the trained Quality Sentinel, we resampled 50 CT scans of the highest label quality from the DAP Atlas to create a new dataset, ensuring a balanced sex distribution (25 male, 25 female) and dividing them into 20 training and 5 testing samples each. This dataset, containing approximately 4 million 2D image-label pairs, has improved training label quality. The stage 2 resampling leads to more accurate ground truth DSC and enhanced model performance, as evidenced in our ablation study in the following section.

Training Details. We opted for ResNet50 as the vision encoder, adjusting its initial layer to accommodate 2-channel inputs. CT HU values were clipped to $[-200, 200]$ and images were cropped and resized to 256×256 around pseudo label centers. These processed pseudo-label masks were then concatenated with the CT images for training. The Quality Sentinel was trained over 30 epochs using the Adam optimizer, with a learning rate of 10^{-3} and batch size of 128. The loss function incorporated a scaling constant $\lambda = 1$. Our experiments were conducted on a PyTorch 2.1.0 framework, utilizing an Intel Xeon Gold 5218R CPU@2.10GHz and 8 Nvidia Quadro RTX 8000 GPUs.

4.2 Evaluation of Quality Sentinel

Ablation Study. To assess the effectiveness of our method, we performed an ablation study concerning text embedding, optimal pair ranking loss, and the data resampling strategy. We utilized three metrics for evaluation: the Linear Correlation Coefficient (LCC), the Spearman Rank Order Correlation Coefficient (SROCC), and the Mean Average Precision (MAP@k), where 'k' refers to the samples with the lowest ground truth DSC. The MAP@k metric is an important ranking metric in our evaluation as it focuses on the samples with the lowest ground truth Dice Similarity Coefficient (DSC), which are cases that may degrade the model training. For each class, the Average Precision at k (AP@k) is first calculated, which involves selecting the k samples with the lowest actual DSC scores and checking if these indices correspond to low predicted scores as well. The precision is accumulated for hits within the top-k ranked predictions, and the MAP@k is computed as the mean AP@k across all classes.

The ablation study is shown in Tab. 1. Incorporating each of the proposed techniques significantly enhances model performance. First, adding class conditions to the model is beneficial for model performance. Even with one-hot embedding of classes, Quality Sentinel performs 2.0% better than

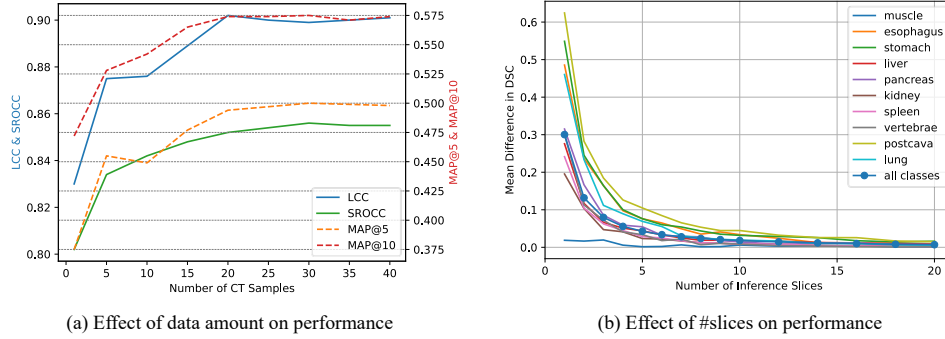


Figure 2: Illustration of (a) the curves of model performance and data amount and (b) the curves of performance deviation *w.r.t.* slice amount compared to prediction with all slices.

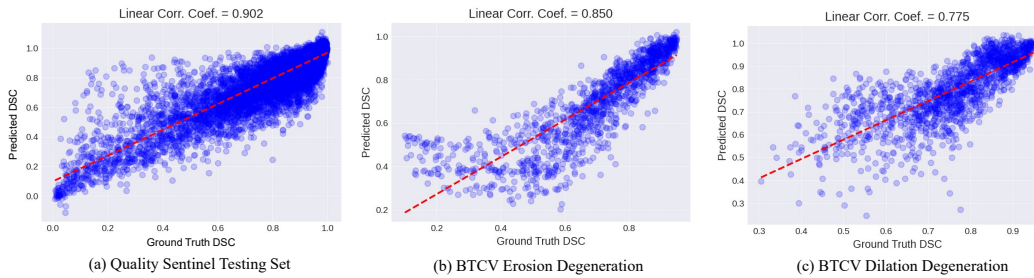


Figure 3: Evaluation of model performance. The scatter plots are illustrated between predicted DSC and ground truth DSC of Quality Sentinel testing set (a) and external evaluation on BTCV with erosion mask degeneration (b) and dilation degeneration (c).

the baseline *w.r.t.* LCC. For different CLIP embeddings, we have tried four different prompt templates. The results show that the best prompt is the simplest one, “[CLS]”. The text embeddings notably improve both regression (*i.e.*, correlation coefficients) and ranking performance (MAP@k). The reason that CLIP embedding performs better than one-hot embedding is that it addresses the label orthogonality problem by exploiting semantic relationships among organs [Liu et al., 2023]. A simpler prompt leads to greater similarity differences between classes, thus eliciting better knowledge from the language. The optimal pair ranking loss is particularly beneficial for ranking (the MAP@10 improved from 0.481 to 0.535 compared to baseline). This would be helpful when using Quality Sentinel to rank sample quality and filter unsatisfying samples. Finally, data resampling markedly boosts all evaluated metrics by enriching the dataset both in volume and quality of ground truth labels.

Evaluation of Model Configurations. The training dataset of Quality Sentinel is obtained from 40 original CT volumes of DAP Atlas. To investigate the impact of training data volume on Quality Sentinel’s efficacy, we analyzed how model performance correlates with the amount of data, represented in Fig. 2 (a). Results indicate performance plateaus at approximately 20-30 CT scans, ensuring the adequacy of our training dataset’s size. In addition, the inference of Quality Sentinel uniformly samples 10 2D slices from a 3D mask, we illustrate the mean difference in DSC *w.r.t.* number of slices used for inference in Fig. 2 (b). The difference between sampling strategy and inference with all slices quickly decreases as the number of slices increases. Specifically, when inferring with 10 slices, the mean difference for all classes is only 0.021, which is acceptable for most practical scenarios.

External Evaluation. Fig. 2 (a) showcases Quality Sentinel’s optimal predictions on its testing set, revealing a strong correlation between the model’s DSC predictions and actual values, underscoring the model’s predictive reliability. However, generalization risks remain since the model was developed on a single data source. We do external evaluations to validate its performance on more data domains. First, we use BTCV [Landman et al., 2015], a well-known manually annotated dataset with 13 classes, to show the model’s performance. As shown in Fig. 2 (b) and (c), we use morpho-

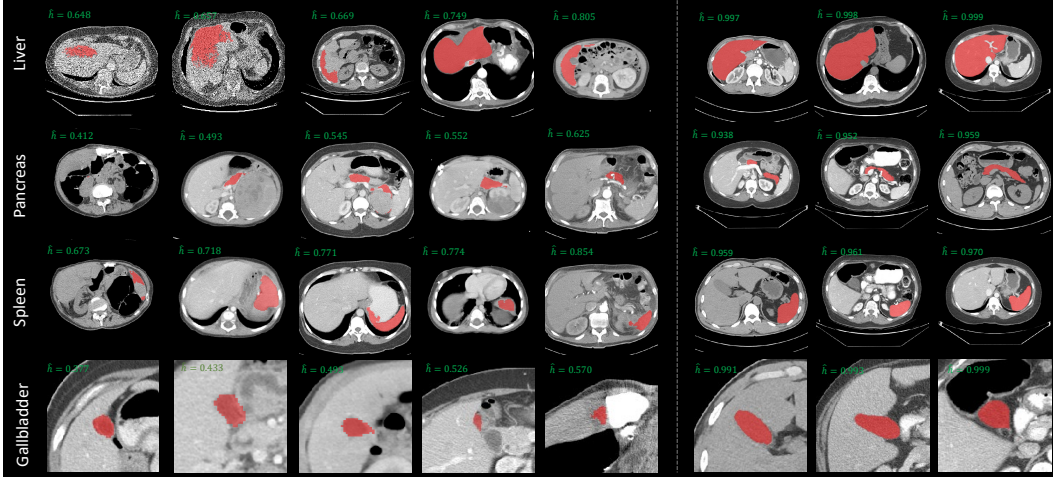


Figure 4: Illustration of labels with lower (left) and higher (right) predicted DSC in AbdomenAtlas dataset. Typical label errors detected include reduced masks (the first two of the liver), missing masks (the first one of the pancreas), and expanded masks (the first three of the gallbladder).

Table 2: Comparison of label quality evaluation for different datasets.

Dataset	# Samples	Annotators	Organ-wise Average Estimation							Overall Estimation		
			aorta	gallbladder	kidney	liver	pancreas	postcava	spleen	stomach	Mean DSC	DSC < 0.8
CHAOS [Valindria et al., 2018]	20	Human	-	-	-	0.985	-	-	-	-	0.985	0.0%
TCIA Pancreas [Roth et al., 2015]	42	Human	-	0.904	0.963	0.961	0.919	-	0.946	0.957	0.941	0.8%
BTCV [Landman et al., 2015]	47	Human	0.943	0.875	0.961	0.981	0.928	0.921	0.962	0.969	0.944	1.7%
AbdomenCT-12organ [Ma et al., 2023]	50	Human	0.965	0.932	0.963	0.965	0.961	0.960	0.964	0.961	0.959	0.0%
WORD [Luo et al., 2021]	120	Human	-	0.874	0.968	0.981	0.946	-	0.958	0.970	0.952	1.9%
LiTS [Bilic et al., 2019]	131	Human	-	-	-	0.963	-	-	-	-	0.963	0.0%
CT-ORG [Rister et al., 2020]	140	Human&AI	-	-	0.911	0.948	-	-	-	-	0.924	0.5%
AMOS22 [Ji et al., 2022]	200	Human&AI	0.954	0.874	0.956	0.971	0.928	0.927	0.953	0.942	0.941	2.1%
KiTS* [Heller et al., 2020]	489	Human	-	-	0.867	-	-	-	-	-	0.867	11.3%
DAP Atlas [Jaus et al., 2023]	533	AI	0.945	0.856	0.946	0.961	0.851	0.919	0.959	0.945	0.925	2.4%
AbdomenCT-1k [Ma et al., 2021]	1000	Human&AI	-	-	0.951	0.963	0.949	-	0.956	-	0.955	0.2%
TotalSegmentator [Wasserthal et al., 2023]	1204	Human&AI	0.927	0.794	0.914	0.941	0.853	0.880	0.933	0.915	0.901	8.0%

* Due to a different annotation protocol of the KiTS dataset, its kidney annotation excludes two tumor types included in it and may account for a relatively large volume, resulting in an underestimated DSC.

logical operations (*i.e.*, erosion and dilation) to generate degraded masks and use Quality Sentinel to infer the DSC, showcasing consistent results with the testing set. Even though the LCC decreases to 0.850 and 0.775 in these two cases, this experiment validates the generalization of Quality Sentinel on out-of-distribution data and unseen mask degradation. We attribute this ability to the large-scale training dataset comprising a wide variety of different degradation modes. Second, we apply Quality Sentinel to the largest multi-organ segmentation dataset, AbdomenAtlas [Qu et al., 2024], to visually demonstrate the model’s ability to detect label errors. In Fig. 4, we show the model prediction of DSCs on four representative abdominal organs. On the left of the figure, imperfect labels with missing, overly expanded, and reduced masks are detected. On the right of the figure, it can be seen that high-quality masks are far smoother and more precise than imperfect masks.

4.3 Dataset Evaluation with Quality Sentinel

Label Quality Comparison. We conducted a comparative analysis of 12 segmentation datasets focusing on major abdominal organs using Quality Sentinel, as detailed in Tab. 2. We observed that smaller datasets, particularly those manually annotated such as AbdomenCT-12organ, a benchmark dataset for the FLARE challenge, exhibit superior organ-wise label quality. Conversely, in larger datasets like TotalSegmentator, where AI-generated pseudo labels are more prevalent, there is a noticeable decline in the overall DSC estimation. Human annotation agreement is usually higher than 0.8 [Qu et al., 2024]. So if considering a quality estimation below 0.8 as inadequate, Quality Sentinel can be used to diagnose the dataset and find the label errors. For instance, it reveals that the TotalSegmentator contains 8% unsatisfying annotations for the abdomen organs and requires potential refinement.

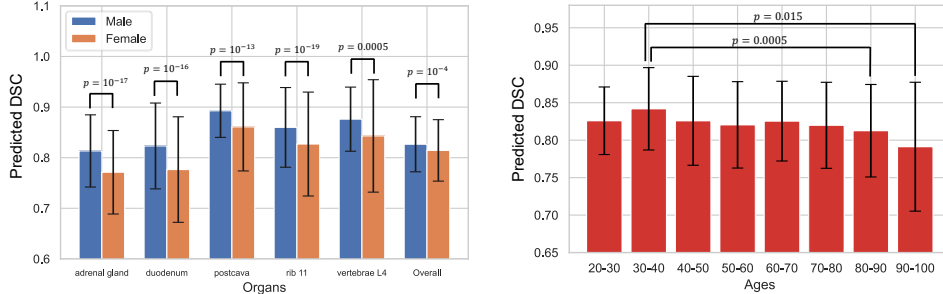


Figure 5: The annotation bias *w.r.t.* gender (left) and age (right) for TotalSegmentator. We show several representative organs with higher label quality for males than females and find a significant overall quality difference for different genders. In addition, older patients generally have worse label quality than younger patients.

Annotation Bias. Investigating the TotalSegmentator dataset, which includes comprehensive meta-data, revealed significant biases in label quality related to gender and age, as illustrated in Fig. 5. Annotations for males and younger individuals were generally of higher quality compared to females and older individuals, with the discrepancies being statistically significant (gender bias $p < 10^{-3}$, age bias $p < 0.05$). These biases may stem from the complexity and severity of conditions in certain patients, which can obscure organ visibility and complicate the annotation. To enhance the generalizability of models for clinical application, future dataset constructions should prioritize more meticulous annotations for these groups.

4.4 Data Efficient Training

In this section, we demonstrate that Quality Sentinel effectively ranks/selects training samples, enhancing the efficiency of training segmentation models. We assessed its performance against random selection, Monte-Carlo Dropout (for diversity) [Gal and Ghahramani, 2016], and Entropy (for uncertainty) [Joshi et al., 2009] on the TotalSegmentator dataset [Wasserthal et al., 2023]. We chose this dataset for its wide range of 104 classes and it is a fair out-of-domain benchmark for comparison. Utilizing a pretrained SwinUNETR [Tang et al., 2022], we fine-tuned the model on 20 full-body CT scans and generated pseudo labels for an additional 100 samples. We then employed these methods to evaluate the quality of pseudo labels, selecting the most suitable samples for further annotating/training, with DSC and Normalized Surface Distance (NSD) serving as the key performance indicators. In the following experiments, the only difference between groups is their selected samples based on different methods.

Human-in-the-Loop (Active Learning). In the human-in-the-loop annotation of datasets, we usually have a small annotation budget, and select a small number of samples that the initial model cannot predict well. These identified samples (namely most informative samples in active learning) are then annotated with human annotators. In our experiment, each method selects n samples based on the lowest pseudo-label quality and revises them with ground truth labels. We combine these samples alongside the original 20 samples for fine-tuning segmentation models. Results (Fig. 6) reveal that Quality Sentinel consistently outperforms the other methods. With a labeling budget of 20 samples, it exceeds random selection by 0.006 and 0.011 in DSC and NSD metrics, respectively. This is comparable to a random selection budget of 30 samples. It means when used for real annotation scenarios, Quality Sentinel can help to reduce about 1/3 annotation cost.

Semi-supervised Learning. In this experiment, we perform a typical semi-supervised learning strategy: self-training with pseudo labels. Each ranking method selects the top 20 pseudo labels with the highest quality. We combine these samples and the initial 20 ground truth-labeled samples to fine-tune The segmentation models. If the selection is not reliable enough and low-quality pseudo-labels are included for training, the model performance may not improve or even be harmed. As Tab. 3 indicates, Quality Sentinel outperforms all alternatives. Specifically, it increases the performance improvement by 33% (0.67% \rightarrow 0.89%) on DSC and 88% (0.41% \rightarrow 0.77%) on NSD compared to the entropy-based method. Compared to random selection, Quality Sentinel has statistically significant improvements ($p = 0.036$ for DSC and $p = 0.0035$ for NSD). As for resource overhead, MC dropout and entropy-based methods need to operate on the 3D raw outputs of the

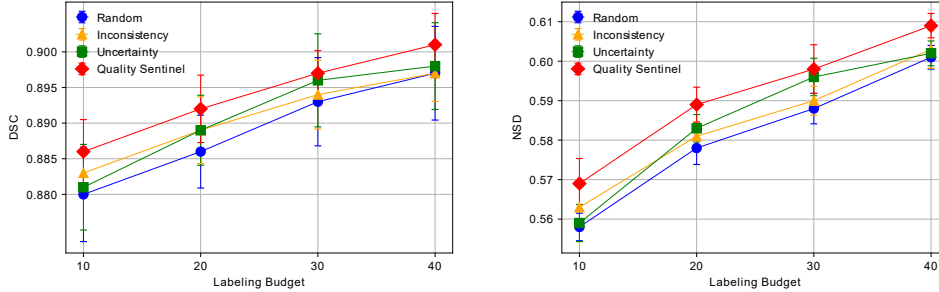


Figure 6: Human-in-the-Loop (active learning) results of label quality ranking methods on the TotalSegmentator. Error bars are reported with 5 repeated experiments. Quality Sentinel helps to reduce annotation costs from 30 samples to 20 samples compared to random selection.

Table 3: Semi-supervised learning results of label quality ranking methods on the TotalSegmentator dataset. Standard deviations are reported with 5 repeated experiments.

Method	# Scans Used		Metrics		Quality Estimation Cost		
	Labeled	Unlabeled	DSC[%]	NSD[%]	Time[h]	RAM[GB]	Disk[GB]
SwinUNETR	20	0	82.55 (± 0.31)	45.76 (± 0.28)	-	-	-
Random	20	100	83.16 (± 0.26)	46.08 (± 0.33)	-	-	-
MC dropout	20	100	83.32 (± 0.57)	46.35 (± 0.46)	3.17	92.4	1032
Entropy	20	100	83.21 (± 0.37)	46.17 (± 0.43)	1.61	33.1	344
Quality Sentinel	20	100	83.44 (± 0.35)	46.53 (± 0.38)	0.50	1.5	0.05

model with the shape $[C, D, H, W]$ and *float* data type. Entropy needs to be computed with per-voxel logits, and MC dropout requires the segmentation model to do inference three times and calculate the standard deviation of each voxel’s probability. In practice, they both require saving the model’s 3D outputs to disk and reloading them to memory for further computation. Instead, Quality Sentinel only needs the segmentation masks with the shape $[D, H, W]$ and the data type of *uint8*. Considering their different compression formats (.npy and .nii.gz), the disk usage can vary by 20,000 times. The 2D processing style and the uniform sampling scheme of Quality Sentinel also largely reduce quality estimation costs (6 times less time and 60 times less RAM than MC dropout).

5 Discussion and Limitations

Quality Sentinel learns generalizable evaluation capability on a large dataset comprising 4M slices. Although it shows good performance on external evaluation, it may not cover all segmentation scenarios. Its training data come from the DAP Atlas dataset with 142 healthy organs. In the KiTS dataset, kidney and kidney tumors are marked as two categories. The definition discrepancy makes the model underestimate label quality (Tab. 2). Moreover, Quality Sentinel is trained on a dataset with balanced gender. Due to the annotation bias discussed before, the different annotation qualities of different groups would possibly affect the ground truth DSC during training. Finally, with Quality Sentinel, it is possible to achieve purposeful QC in data sets. On the one hand, it can help improve the annotation and balance of the data set, but on the other hand, there is also the risk of being exploited to intentionally control the preferences of the data and model.

6 Conclusion

Our primary contribution is the development of Quality Sentinel, a label quality estimation model trained on a vast and diverse set of image-label pairs. This model enables a thorough evaluation of dataset quality and identification of biases. It acts as a pivotal tool for sample selection, both for guiding human-in-the-loop annotation and for model training. While our empirical results show the practical value of the model on CT images, an important future work is to extend Quality Sentinel to more modalities to be a generic label evaluator for medical image segmentation. We envision that Quality Sentinel will play a crucial role in quality control for expansive datasets, thereby enhancing training efficiency and applicability in real-world scenarios.

References

- Xenia Alba, Karim Lekadir, Marco Pereanez, Pau Medrano-Gracia, Alistair A Young, and Alejandro F Frangi. Automatic initialization and quality control of large-scale cardiac mri segmentations. *Medical image analysis*, 43:129–141, 2018.
- Patrick Bilic, Patrick Ferdinand Christ, Eugene Vorontsov, Grzegorz Chlebus, Hao Chen, Qi Dou, Chi-Wing Fu, Xiao Han, Pheng-Ann Heng, Jürgen Hesser, et al. The liver tumor segmentation benchmark (lits). *arXiv preprint arXiv:1901.04056*, 2019.
- Tom Brown, Benjamin Mann, Nick Ryder, Melanie Subbiah, Jared D Kaplan, Prafulla Dhariwal, Arvind Neelakantan, Pranav Shyam, Girish Sastry, Amanda Askell, et al. Language models are few-shot learners. *NeurIPS*, 33:1877–1901, 2020.
- Samuel Budd, Emma C Robinson, and Bernhard Kainz. A survey on active learning and human-in-the-loop deep learning for medical image analysis. *Medical Image Analysis*, 71:102062, 2021.
- Jieneng Chen, Yongyi Lu, Qihang Yu, Xiangde Luo, Ehsan Adeli, Yan Wang, Le Lu, Alan L Yuille, and Yuyin Zhou. Transunet: Transformers make strong encoders for medical image segmentation. *arXiv preprint arXiv:2102.04306*, 2021.
- David F Crouse. On implementing 2d rectangular assignment algorithms. *IEEE Transactions on Aerospace and Electronic Systems*, 52(4):1679–1696, 2016.
- Aron Culotta and Andrew McCallum. Reducing labeling effort for structured prediction tasks. In *AAAI*, volume 5, pages 746–751, 2005.
- Jacob Devlin, Ming-Wei Chang, Kenton Lee, and Kristina Toutanova. Bert: Pre-training of deep bidirectional transformers for language understanding. In *NAACL*, pages 4171–4186, 2019.
- Terrance DeVries and Graham W Taylor. Leveraging uncertainty estimates for predicting segmentation quality. *arXiv preprint arXiv:1807.00502*, 2018.
- Sedigheh Eslami, Christoph Meinel, and Gerard De Melo. Pubmedclip: How much does clip benefit visual question answering in the medical domain? In *EACL*, pages 1181–1193, 2023.
- Joris Fournel, Axel Bartoli, David Bendahan, Maxime Guye, Monique Bernard, Elisa Rausero, Mohammed Y Khanji, Steffen E Petersen, Alexis Jacquier, and Badih Ghattas. Medical image segmentation automatic quality control: A multi-dimensional approach. *Medical Image Analysis*, 74:102213, 2021.
- Yarin Gal and Zoubin Ghahramani. Dropout as a bayesian approximation: Representing model uncertainty in deep learning. In *ICML*, pages 1050–1059. PMLR, 2016.
- Yarin Gal, Riashat Islam, and Zoubin Ghahramani. Deep bayesian active learning with image data. In *ICML*, pages 1183–1192. PMLR, 2017.
- Francesco Galati, Sébastien Ourselin, and Maria A Zuluaga. From accuracy to reliability and robustness in cardiac magnetic resonance image segmentation: a review. *Applied Sciences*, 12(8):3936, 2022.
- Adrian Galdran, Pedro Costa, Alessandro Bria, Teresa Araújo, Ana Maria Mendonça, and Aurélio Campilho. A no-reference quality metric for retinal vessel tree segmentation. In *MICCAI*, pages 82–90. Springer, 2018.
- Ali Hatamizadeh, Yucheng Tang, Vishwesh Nath, Dong Yang, Andriy Myronenko, Bennett Landman, Holger R Roth, and Daguang Xu. Unetr: Transformers for 3d medical image segmentation. In *WACV*, pages 574–584, 2022.
- Kaiming He, Xiangyu Zhang, Shaoqing Ren, and Jian Sun. Deep residual learning for image recognition. In *CVPR*, pages 770–778, 2016.
- Nicholas Heller, Sean McSweeney, Matthew Thomas Peterson, Sarah Peterson, Jack Rickman, Bethany Stai, Resha Tejpaul, Makinna Oestreich, Paul Blake, Joel Rosenberg, et al. An international challenge to use artificial intelligence to define the state-of-the-art in kidney and kidney tumor segmentation in ct imaging., 2020.

- Chao Huang, Qingbo Wu, and Fanman Meng. Qualitynet: Segmentation quality evaluation with deep convolutional networks. In *VCIP*, pages 1–4. IEEE, 2016.
- Ziyan Huang, Haoyu Wang, Zhongying Deng, Jin Ye, Yanzhou Su, Hui Sun, Junjun He, Yun Gu, Lixu Gu, Shaoting Zhang, et al. Stu-net: Scalable and transferable medical image segmentation models empowered by large-scale supervised pre-training. *arXiv preprint arXiv:2304.06716*, 2023.
- Fabian Isensee, Paul F Jaeger, Simon AA Kohl, Jens Petersen, and Klaus H Maier-Hein. nnu-net: a self-configuring method for deep learning-based biomedical image segmentation. *Nature methods*, 18(2):203–211, 2021.
- Alexander Jaus, Constantin Seibold, Kelsey Hermann, Alexandra Walter, Kristina Giske, Johannes Haubold, Jens Kleesiek, and Rainer Stiefelwagen. Towards unifying anatomy segmentation: automated generation of a full-body ct dataset via knowledge aggregation and anatomical guidelines. *arXiv preprint arXiv:2307.13375*, 2023.
- Yuanfeng Ji, Haotian Bai, Jie Yang, Chongjian Ge, Ye Zhu, Ruimao Zhang, Zhen Li, Lingyan Zhang, Wanling Ma, Xiang Wan, et al. Amos: A large-scale abdominal multi-organ benchmark for versatile medical image segmentation. *arXiv preprint arXiv:2206.08023*, 2022.
- Ajay J Joshi, Fatih Porikli, and Nikolaos Papanikolopoulos. Multi-class active learning for image classification. In *CVPR*, pages 2372–2379. IEEE, 2009.
- Bennett Landman, Zhoubing Xu, J Igelsias, Martin Styner, T Langerak, and Arno Klein. Miccai multi-atlas labeling beyond the cranial vault—workshop and challenge. In *Proc. MICCAI Multi-Atlas Labeling Beyond Cranial Vault—Workshop Challenge*, volume 5, page 12, 2015.
- Wenxuan Li, Alan Yuille, and Zongwei Zhou. How well do supervised models transfer to 3d image segmentation? In *The Twelfth International Conference on Learning Representations*, 2023.
- Xin Li and Yuhong Guo. Adaptive active learning for image classification. In *CVPR*, pages 859–866, 2013.
- Qiao Lin, Xin Chen, Chao Chen, and Jonathan M Garibaldi. A novel quality control algorithm for medical image segmentation based on fuzzy uncertainty. *IEEE Transactions on Fuzzy Systems*, 2022.
- Jie Liu, Yixiao Zhang, Jie-Neng Chen, Junfei Xiao, Yongyi Lu, Bennett A Landman, Yixuan Yuan, Alan Yuille, Yucheng Tang, and Zongwei Zhou. Clip-driven universal model for organ segmentation and tumor detection. In *ICCV*, pages 21152–21164, 2023.
- Benedikt Lorch, Ghislain Vaillant, Christian Baumgartner, Wenjia Bai, Daniel Rueckert, and Andreas Maier. Automated detection of motion artefacts in mr imaging using decision forests. *Journal of medical engineering*, 2017, 2017.
- Xiangde Luo, Wenjun Liao, Jianghong Xiao, Tao Song, Xiaofan Zhang, Kang Li, Guotai Wang, and Shaoting Zhang. Word: Revisiting organs segmentation in the whole abdominal region. *arXiv preprint arXiv:2111.02403*, 2021.
- Jun Ma, Yao Zhang, Song Gu, Cheng Zhu, Cheng Ge, Yichi Zhang, Xingle An, Congcong Wang, Qiyuan Wang, Xin Liu, et al. Abdomenct-1k: Is abdominal organ segmentation a solved problem. *IEEE Transactions on Pattern Analysis and Machine Intelligence*, 2021.
- Jun Ma, Yao Zhang, Song Gu, Cheng Ge, Shihao Ma, Adamo Young, Cheng Zhu, Kangkang Meng, Xin Yang, Ziyan Huang, et al. Unleashing the strengths of unlabeled data in pan-cancer abdominal organ quantification: the flare22 challenge. *arXiv preprint arXiv:2308.05862*, 2023.
- Dwarikanath Mahapatra, Behzad Bozorgtabar, Jean-Philippe Thiran, and Mauricio Reyes. Efficient active learning for image classification and segmentation using a sample selection and conditional generative adversarial network. In *International Conference on Medical Image Computing and Computer-Assisted Intervention*, pages 580–588. Springer, 2018.

- Ilkay Oksuz, Bram Ruijsink, Esther Puyol-Antón, James R Clough, Gastao Cruz, Aurelien Bustin, Claudia Prieto, Rene Botnar, Daniel Rueckert, Julia A Schnabel, et al. Automatic cnn-based detection of cardiac mr motion artefacts using k-space data augmentation and curriculum learning. *Medical image analysis*, 55:136–147, 2019.
- Ozan Oktay, Jo Schlemper, Loic Le Folgoc, Matthew Lee, Mattias Heinrich, Kazunari Misawa, Kensaku Mori, Steven McDonagh, Nils Y Hammerla, Bernhard Kainz, et al. Attention u-net: Learning where to look for the pancreas. *arXiv preprint arXiv:1804.03999*, 2018.
- Ziyuan Qin, Huahui Yi, Qicheng Lao, and Kang Li. Medical image understanding with pretrained vision language models: A comprehensive study. *arXiv preprint arXiv:2209.15517*, 2022.
- Chongyu Qu, Tiezheng Zhang, Hualin Qiao, Yucheng Tang, Alan L Yuille, Zongwei Zhou, et al. Abdomenatlas-8k: Annotating 8,000 ct volumes for multi-organ segmentation in three weeks. *Advances in Neural Information Processing Systems*, 36, 2024.
- Alec Radford, Jong Wook Kim, Chris Hallacy, Aditya Ramesh, Gabriel Goh, Sandhini Agarwal, Girish Sastry, Amanda Askell, Pamela Mishkin, Jack Clark, et al. Learning transferable visual models from natural language supervision. In *ICML*, pages 8748–8763. PMLR, 2021.
- Blaine Rister, Darvin Yi, Kaushik Shivakumar, Tomomi Nobashi, and Daniel L Rubin. Ct-org, a new dataset for multiple organ segmentation in computed tomography. *Scientific Data*, 7(1):1–9, 2020.
- Robert Robinson, Ozan Oktay, Wenjia Bai, Vanya V Valindria, Mihir M Sanghvi, Nay Aung, José M Paiva, Filip Zemrak, Kenneth Fung, Elena Lukaschuk, et al. Real-time prediction of segmentation quality. In *MICCAI*, pages 578–585. Springer, 2018.
- Olaf Ronneberger, Philipp Fischer, and Thomas Brox. U-net: Convolutional networks for biomedical image segmentation. In *MICCAI*, pages 234–241. Springer, 2015.
- Holger R Roth, Le Lu, Amal Farag, Hoo-Chang Shin, Jiamin Liu, Evrim B Turkbey, and Ronald M Summers. Deeporgan: Multi-level deep convolutional networks for automated pancreas segmentation. In *MICCAI*, pages 556–564. Springer, 2015.
- Yucheng Tang, Dong Yang, Wenqi Li, Holger R Roth, Bennett Landman, Daguang Xu, Vishwesh Nath, and Ali Hatamizadeh. Self-supervised pre-training of swin transformers for 3d medical image analysis. In *CVPR*, pages 20730–20740, 2022.
- Giacomo Tarroni, Ozan Oktay, Wenjia Bai, Andreas Schuh, Hideaki Suzuki, Jonathan Passerat-Palmbach, Antonio De Marvao, Declan P O’Regan, Stuart Cook, Ben Glocker, et al. Learning-based quality control for cardiac mr images. *IEEE transactions on medical imaging*, 38(5):1127–1138, 2018.
- Constantin Ulrich, Fabian Isensee, Tassilo Wald, Maximilian Zenk, Michael Baumgartner, and Klaus H Maier-Hein. Multitalent: A multi-dataset approach to medical image segmentation. In *MICCAI*, pages 648–658. Springer, 2023.
- Vanya V Valindria, Nick Pawlowski, Martin Rajchl, Ioannis Lavdas, Eric O Aboagye, Andrea G Rockall, Daniel Rueckert, and Ben Glocker. Multi-modal learning from unpaired images: Application to multi-organ segmentation in ct and mri. In *WACV*, pages 547–556. IEEE, 2018.
- Zifeng Wang, Zhenbang Wu, Dinesh Agarwal, and Jimeng Sun. Medclip: Contrastive learning from unpaired medical images and text. In *EMNLP*, 2022.
- Jakob Wasserthal, Hanns-Christian Breit, Manfred T Meyer, Maurice Pradella, Daniel Hinck, Alexander W Sauter, Tobias Heye, Daniel T Boll, Joshy Cyriac, Shan Yang, et al. Totalsegmentator: Robust segmentation of 104 anatomic structures in ct images. *Radiology: Artificial Intelligence*, 5(5), 2023.
- Donggeun Yoo and In So Kweon. Learning loss for active learning. In *CVPR*, pages 93–102, 2019.
- Fahim Ahmed Zaman, Lichun Zhang, Honghai Zhang, Milan Sonka, and Xiaodong Wu. Segmentation quality assessment by automated detection of erroneous surface regions in medical images. *Computers in biology and medicine*, 164:107324, 2023.

Zhenxi Zhang, Jie Li, Chunna Tian, Zhusi Zhong, Zhicheng Jiao, and Xinbo Gao. Quality-driven deep active learning method for 3d brain mri segmentation. *Neurocomputing*, 446:106–117, 2021.

Tianfei Zhou, Liulei Li, Gustav Bredell, Jianwu Li, Jan Unkelbach, and Ender Konukoglu. Volumetric memory network for interactive medical image segmentation. *Medical Image Analysis*, 83:102599, 2023.